Magnetic interactions in epitaxial films of Mn5(Ge1-xSix)3/Ge(111) : 55Mn NMR study

R. Kalvig, E. Jędryka, S. Kang, M. Petit, L. Michez, M. Wójcik

Journal of Magnetism and Magnetic Materials 600 (2024) 172120

Contents lists available at ScienceDirect

Journal of Magnetism and Magnetic Materials

journal homepage: www.elsevier.com/locate/jmmm

Research article

Magnetic interactions in epitaxial films of $Mn_5(Ge_{1-x}Si_x)_3$/Ge(111) : ^{55}Mn NMR study

R. Kalvig [a], E. Jędryka [a,*], S. Kang [b], M. Petit [b], L. Michez [b], M. Wójcik [a]

[a] Institute of Physics, Polish Academy of Sciences, Aleja Lotnikow 32/46, Warsaw, PL-02668, Poland
[b] Aix-Marseille Univ, CNRS, CINAM, Marseille, France

ARTICLE INFO

Keywords:
Thin films
NMR
$Mn_5(GeSi)_3$
Magnetic structure
Magnetic moments

ABSTRACT

^{55}Mn NMR experiments have been performed at 4.2 K on a series of $Mn_5(Ge_{1-x}Si_x)_3$ epitaxial films ($0 \leqslant x \leqslant 0.55$) to investigate changes introduced by silicon when it replaces germanium in a hexagonal Mn_5Ge_3 crystal lattice. The Si/Ge substitution was found to reduce the magnetic moment on manganese located in the 6(g) sublattice creating a new population of manganese atoms with distinctly lower magnetic moment. This effect is attributed to the orbital overlay due to a lattice distortion introduced by Si. Interestingly, these modified Mn sites retain the orbital moment practically unaltered. The amount of new manganese environments in the 6(g) sublattice coincides with a probability of Mn having two Si neighbors as first neighbors. Mn atoms located in the 4(d) sublattice are not significantly affected by the Si substitution in the studied concentration range.

1. Introduction

Magnetic interactions at low temperatures in the antiferromagnetic Mn_5Si_3 compound give rise to many interesting phenomena, such as the topological Hall effect [1] and inverse magnetocaloric effect [2]. Recent reports indicate that the epitaxial films of Mn_5Si_3 show particular features that were not observed in the bulk form, such as anisotropic anomalous Hall effect [3] indicating the presence of altermagnetism in these structures [4]. These findings have induced a lot of renewed research interest in the epitaxial films of Mn_5Si_3 [5]. A complex magnetic structure of Mn_5Si_3 is defined by two first-order transitions as a function of temperature. A collinear spin arrangement (AF2) observed below the Neél point (T_N = 99 K) becomes frustrated at 65 K, resulting in the non-collinear magnetic structure (AF1) the details of which are still a subject of debate [6,7]. On the other hand, the isostructural Mn_5Ge_3 compound is a metallic ferromagnet with the Curie temperature of 296 K [8]. Mn_5Ge_3 and Mn_5Si_3 crystallize in the hexagonal $D8_8$ structure (space-group $P6_3/mcm$) and in the bulk form they can be mutually alloyed over the entire concentration range. Recent report communicates a successful growth of the high quality epitaxial films of $Mn_5(Ge_{1-x}Si_x)_3$ with uniform characteristics for the concentration range $0 < x < 0.6$ [9]. This has opened an unique opportunity to follow step by step the modification introduced by Si substitution to the ferromagnetic interactions in epitaxial films of pristine Mn_5Ge_3. In this work we have undertaken the ^{55}Mn NMR study at 4.2 K in a series of $Mn_5(Ge_{1-x}Si_x)_3$ epitaxial films ($0 \leqslant x \leqslant 0.55$). We show that progressive replacement of Ge with Si atoms affects hyperfine fields on ^{55}Mn nuclei due to orbital overlay introduced by a lattice distortion. We find that the Si/Ge substitution reduces the magnetic moment on those Mn_{II} atoms that happen to have at least two Si neighbors as first neighbors, creating a new population of the Mn_{II} atoms with distinctly lower magnetic moment. Interestingly, these new Mn_{II} environments retain their orbital moment practically unaltered. On the other hand, the Mn_I atoms located in the 4(d) position are not locally affected by the Si substitution, and experience only an indirect effect of the reduced average magnetic moment of the sample. These results shed new light on the NMR experiment in the $Mn_5(Ge_{1-x}Si_x)_3$ system, partly contradicting the previous report of a different group [10], which was based on a study of the bulk (polycrystalline) specimens. Here, we take advantage of the availability of the high quality epitaxial films, allowing for a precise orientation with respect to the external magnetic field and providing a correct interpretation of the NMR signal. The comparative discussion is presented in Section 4.

2. Experimental

A series of $Mn_5(Ge_{1-x}Si_x)_3$ epitaxial films (x = 0.0, 0.05, 0.1, 0.2, 0.3, 0.4, and 0.55) with a nominal thickness of 60 nm has been grown on the Ge(111) substrate using molecular beam epitaxy (MBE). The epitaxial relationship is such that the (001) Mn_5Ge_3 ‖ (111) Ge and [010] Mn_5Ge_3 ‖ [11-2] Ge, therefore the hexagonal c-plane lies in the plane of the film. Prior to deposition the Ge(111) substrates were

* Corresponding author.
E-mail address: jedry@ifpan.edu.pl (E. Jędryka).

https://doi.org/10.1016/j.jmmm.2024.172120
Received 25 March 2024; Received in revised form 24 April 2024; Accepted 4 May 2024
Available online 7 May 2024

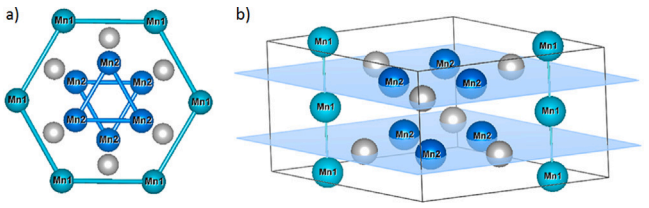

Fig. 1. Unit cell of Mn_5Ge_3: (a) top view on the hexagonal plane; (b) side view. Colored spheres represent atoms: (Mn_I (green), Mn_{II} (blue), Ge/Si (gray). This drawing was prepared using the VESTA software [13].

subjected to a chemical cleaning and annealing. The growth process was controlled by in-situ reflection high-energy electron diffraction (RHEED) using a beam acceleration voltage of 30 kV. A full description of sample preparation details can be found in Ref. [9].

^{55}Mn Nuclear Magnetic Resonance (NMR) experiments were performed at 4.2 K with the use of an automatic, phase-sensitive spin-echo spectrometer. The spectra have been recorded in the frequency-swept mode, in zero field as well as in the presence of a constant external magnetic field. The experiments were performed in the frequency range 150–500 MHz with the 1 MHz step at several values of the r.f. field amplitude. The optimum amplitude of the spin-echo signal as well as the NMR enhancement factor at each frequency have been computed according to the Panissod protocol [11]. The final spectra have been subsequently corrected for the frequency variation of the NMR enhancement factor and represent a true distribution of signal intensity.

The NMR resonance frequency ν is a very sensitive probe of the magnetic moments in different lattice sites. It is determined by the effective magnetic-field B_{eff} at the site of the nucleus:

$$\nu = \gamma|\vec{B}_{eff}| \approx \gamma|\vec{B}_{hf} + \vec{B}_{ext}| \quad (1)$$

where γ denotes the nuclear gyromagnetic ratio and $\vec{B}_{eff}$ is the effective magnetic field, consisting of the external field $\vec{B}_{ext}$ and the hyperfine field $\vec{B}_{hf}$ generated at the nucleus by the surrounding electrons and magnetic dipoles. A full description of all contributions to the internal magnetic fields in the studied compounds has been given in Ref. [12].

3. Results and discussion

The hexagonal unit cell of Mn_5Ge_3 and Mn_5Si_3 contains two formula units, with the manganese atoms located in the two respective Wyckoff crystallographic positions: 4(d) and 6(g) (traditionally denoted as Mn_I and Mn_{II} sites), as shown in Fig. 1.

3.1. Basic features of ^{55}Mn NMR in the two manganese lattice sites of Mn_5Ge_3

The NMR features in the epitaxial film with a pristine Mn_5Ge_3 composition ($x = 0$) have been a subject of our previous reports, providing a wealth of information on the local magnetic properties of manganese in this structure [12,14]. Fig. 2 presents the zero-field ^{55}Mn NMR spectrum recorded at 4.2 K from the $x = 0$ sample of the present series.

The two NMR lines centered around 208.2 MHz (Mn_I site) and 429.8 MHz (Mn_{II} site) correspond to the hyperfine field (B_{hf}) value of 19.73 T and 40.73 T, respectively. Such a large difference of hyperfine fields reflects the significantly different magnetic moments of manganese in the two lattice sites, according to the well-known formula [15]

$$\vec{B}_{hf} \approx \vec{B}^{cf}_{hf} + \vec{B}^{orb}_{hf} = A^{cf}\vec{\mu}_s + A^{orb}\vec{\mu}_{orb} \quad (2)$$

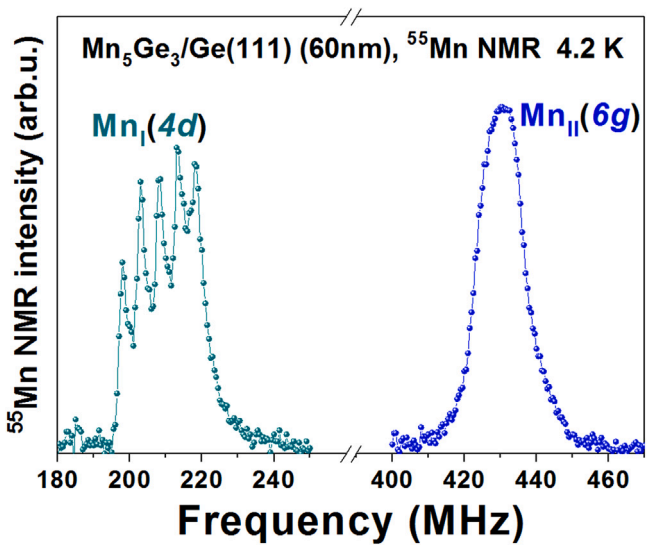

Fig. 2. Zero-field ^{55}Mn NMR spectrum recorded from the 60 nm thick Mn_5Ge_3 epitaxial film at 4.2 K. Green and blue symbols denote the NMR signals from Mn_I and Mn_{II} lattices, respectively.

where $\vec{\mu}_s$ and $\vec{\mu}_{orb}$ denote spin and orbital moment whereas A^{cf} and A^{orb} are the respective components of the hyperfine interaction constant. The proposed assigment of the NMR lines is fully consistent with the previous neutron diffraction study reporting the magnetic moment values of 1.96(3) μ_B (Mn_I site) and 3.23(2) μ_B (Mn_{II} site) [16].

Our previous NMR study revealed also a significant contribution of the unquenched Mn orbital magnetic moment ($\vec{\mu}_{orb}$) in both crystalline sites, giving rise to a large anisotropy of the ^{55}Mn hyperfine field value between the hexagonal c-plane and c-axis: 1.52 T in the 4(d) site and up to 4 T in the 6(g) site – the latter was additionally modulated as a function of orientation within the c-plane [12]. The 4(d) site has uniaxial symmetry and a strong electric field gradient (EFG) oriented along the hexagonal c-axis, leading to a well-resolved quadrupolar structure of the corresponding NMR line. It is well established that a quadrupolar interaction between the electric quadrupole moment of a nucleus (Q) and the electric field gradient (eq) produced by the local nuclear and electronic charges, splits the NMR line into $2I$ components (nuclear spin of ^{55}Mn I = 5/2). The separation between individual components of a quadrupolar structure is given by [17]:

$$\Delta\nu = \frac{1}{2}\nu_Q(m - \frac{1}{2})(cos^2\theta - 1) \quad (3)$$

where the quadrupolar frequency ν_Q is defined as $\nu_Q = \frac{3e^2qQ}{2I(2I-1)h}$ and θ is the angle between the EFG and a local magnetization.

3.2. The effect of Si/Ge replacement on manganese in the 4(d) lattice site

Let us first consider the effect of Si on the NMR spectrum corresponding to the Mn_I site, shown in Fig. 3. Here the effect of increasing Si concentration is not very strong - it consists in a systematic, quasi-linear downshift of a broad NMR line (central frequency of the quadrupolar structure is indicated with the red arrow). Another observation that can be made is a slow linear increase of separation between the quadrupolar components as shown in Fig. 4, leading to a progressive line broadening and a loss of resolution. Bearing in mind that the quadrupolar frequency is proportional to the electric field gradient (see Eq. (2)), the observed broadening of the quadrupolar components can be readily attributed to a lattice distortion caused by the Ge replacement with Si. Due to a smaller atomic size of Si compared to Ge, the lattice parameters of Mn_5Si_3 are reduced with respect to Mn_5Ge_3 and the unit cell is uniformly compressed. In the mixed $Mn_5(GeSi)_3$

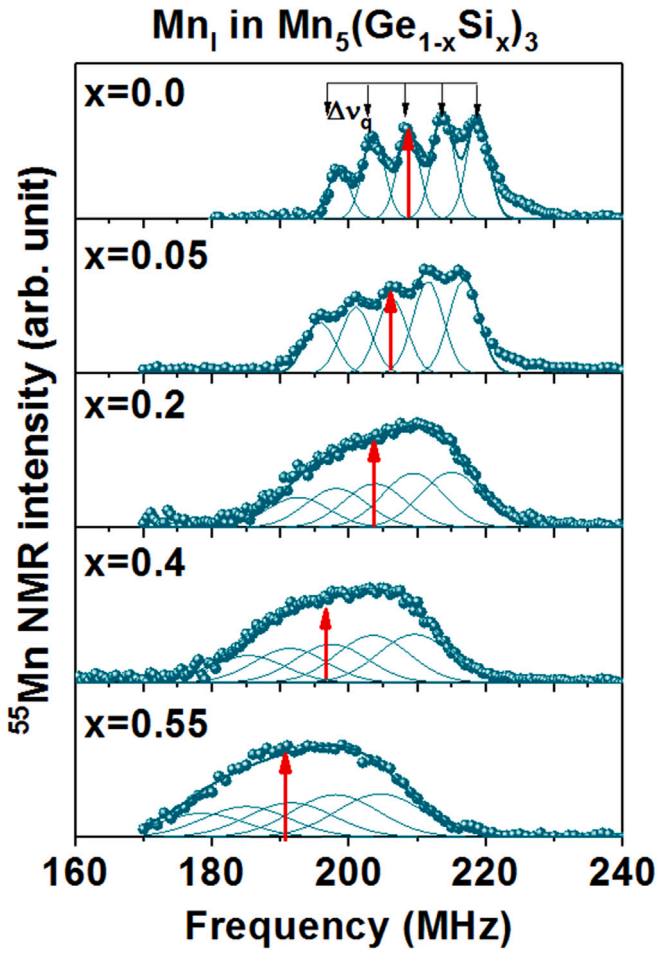

Fig. 3. Zero-field ^{55}Mn NMR spectra recorded from the Mn$_I$ sublattice in a series of Mn$_5$(Ge$_{1-x}$Si$_x$)$_3$ epitaxial films. For $x \geqslant 0.2$ a fit was applied to reconstruct the lost resolution of a quadrupolar structure. Red arrows indicate the central line position.

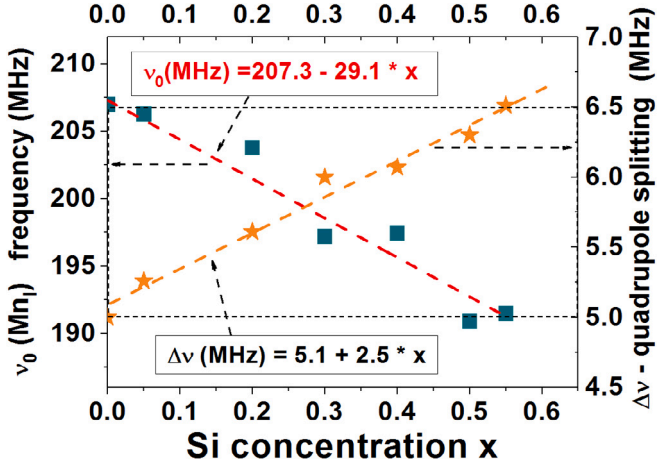

Fig. 4. ^{55}Mn NMR in the Mn$_I$ sublattice as a function of Si concentration. Green squares: central line frequency; orange stars: frequency separation of the quadrupolar components.

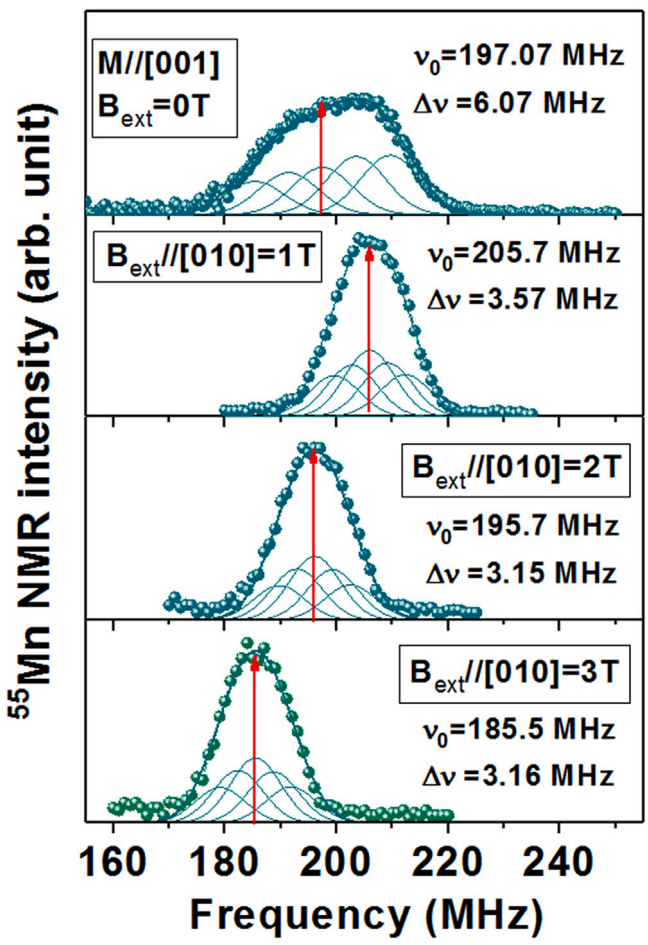

Fig. 5. ^{55}Mn NMR spectra (Mn$_I$ sublattice) recorded from the Mn$_5$(Ge$_{0.6}$Si$_{0.4}$)$_3$ film in the external in-plane field varying between 0 and 3 T.

systems this entails a local lattice distortion and a non-uniform electric field gradient. As already mentioned, a pristine Mn_5Ge_3 film displayed a strong anisotropy of manganese orbital moment in the Mn$_I$ site leading to a difference of 1.52 T between the hyperfine field measured along the c-axis with respect to any direction in the c-plane [14]. To find out whether the Si/Ge replacement affects the anisotropic properties, we performed experiments in presence of an external magnetic field applied in the film plane. The NMR spectra corresponding to the Mn$_I$ sublattice are shown in Fig. 5 as a function of the in-plane varying between 0 and 3 T.

With increasing the in-plane field strength we observe an initial upshift of the NMR line and around 0.5 T - a linear drop of the NMR frequency with a slope determined by the ^{55}Mn gyromagnetic ratio (γ = 10.5 MHz/T) - see Fig. 6. This means that in the demagnetized state the magnetization is oriented out-of-plane and the field of around 0.5 T is needed to overcome the magnetocrystalline anisotropy and reach the in-plane orientation. Once all the spins are in plane, the external field acts along the electronic magnetization. Further increase of the external field strength reduces the hyperfine field (and consequently the NMR frequency), since a hyperfine field is oriented opposite to the magnetization. The initial upshift of NMR frequency is an evidence that in a sample with $x = 0.4$ the anisotropy of manganese orbital moment in the Mn$_I$ site still persists, similar to that observed previously in a pristine Mn_5Ge_3 film [14]. Another evidence that the NMR signal from a sample with $x = 0.4$ is observed along the c-axis is a drop of the NMR linewidth due to a reduced separation between the quadrupolar components from $\Delta\nu = 6.07$ MHz (along the c-direction, $\theta = 0°$) down to $\Delta\nu = 3.15$ MHz (in the c-plane, $\theta = 90°$), as shown in Fig. 5. This effect is similar to that observed in the pristine film [14] and comes from the varying angle θ between the magnetization and the EFG, according to Eq. (2). The zero-field value of $\Delta\nu$ is approximately twice as large as that for the c-plane, which was also the case for the pristine

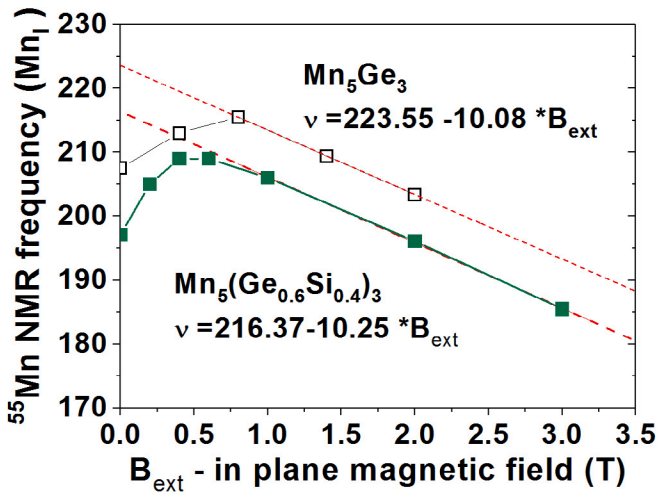

Fig. 6. In-plane field dependence of the Mn_I NMR line (central frequency) for $x = 0$ (empty back squares) and $x = 0.4$ (green squares).

film. Clearly, up to 55% of Si content no significant modification of the local magnetic properties of manganese in the 4(d) lattice site have been observed. The NMR spectrum from the Mn_I lattice reflects only a slight drop of the average magnetization, due to a reduced transferred hyperfine field component.

3.3. The effect of Si/Ge replacement on manganese in the 6(g) lattice site

A systematic downshift of the NMR spectrum as a function of silicon content is observed also in the case of Mn_{II} site, as shown in Fig. 7.

In addition, the NMR spectrum from Mn_{II} sites develops a broad low frequency profile (satellite line) revealing the presence of a new population (Mn_{IInew}) with a significantly reduced magnetic moment. The NMR frequency of satellite line decreases faster than the main line – the frequency separation between the two spectrum components rapidly increases with Si concentration (see Fig. 8). This shows that Si substitution for Ge entails a systematic drop of manganese magnetic moment in the 6(g) lattice sites.

To determine the respective orientation of spins giving rise to the Mn_{II} and Mn_{IInew} NMR signals we performed experiments applying the external magnetic field parallel to the film normal i.e. along the hexagonal c-direction of the crystals. Fig. 9 presents the NMR spectra recorded from the film with $x = 0.4$ at zero field and in the field 1 T and 3 T, showing no change between 0 and 1 T in either (Mn_I and Mn_{II}) crystal site.

This means that for the concentration $x = 0.4$ the NMR signal originates from spins oriented along the film normal and the effect of a small external field is shielded by the domain structure, similar to the case of a thicker film with $x = 0$ previously reported [14]. At higher external field values the sample becomes magnetically saturated and the external field acts along the electronic magnetization i.e. opposite to the hyperfine field on a nucleus. This leads to a downshift of the NMR frequency. As shown in the Fig. 10, the NMR frequency of all three NMR lines shifts linearly in presence of the out-of-plane field with a slope close to the gyromagnetic ratio of ^{55}Mn, revealing that the magnetic moments contributing to these signals are parallel and ferromagnetically coupled in the studied concentration range. This means that the lower NMR frequency in the Mn_{IInew} environments is not due to the changed orientation, but rather to a new absolute value of magnetic moment on those lattice sites. Mn_{II} atoms are located at the same atomic plane as Si/Ge (cf Fig. 1b), so it is to be expected that the modification of interatomic distances due to Si replacing Ge will alter the exchange interactions in the 6(g) sublattice. Evidently, this

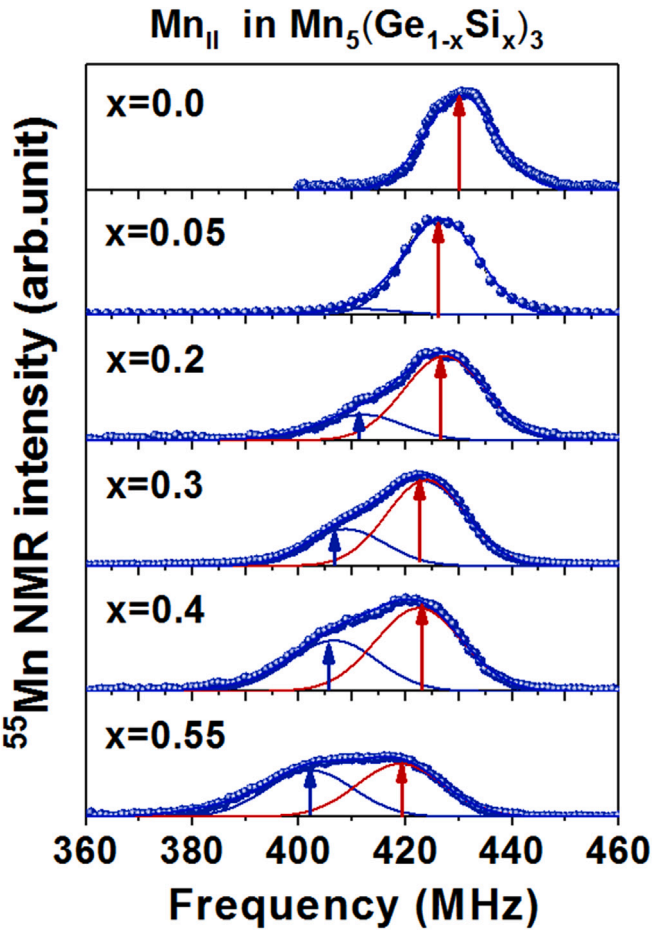

Fig. 7. Zero-field ^{55}Mn NMR spectra recorded from the Mn_{II} sublattice in a series of $Mn_5(Ge_{1-x}Si_x)_3$ epitaxial films ($0 \leqslant x \leqslant 0.55$). Red arrows indicate the NMR frequency of the original Mn_{II} line and blue arrows - the satellite line originating from the modified Mn_{II} environments.

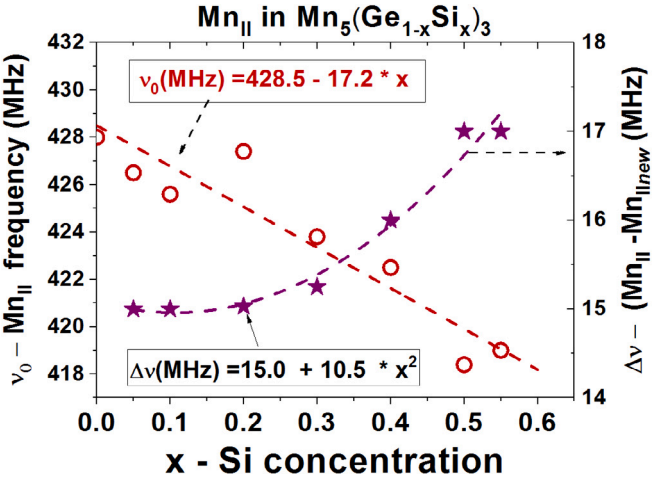

Fig. 8. ^{55}Mn NMR in the Mn_{II} sublattice as a function of Si concentration. Red open circles-NMR frequency of the original Mn_{II} line; purple stars: frequency separation between the Mn_{II} and Mn_{IInew} NMR lines.

leads to a drop of the local magnetic moment on those Mn_{II} atoms that have Si instead of Ge as the nearest neighbors (nn).

Assuming a random (binomial) distribution of Si atoms over the crystal lattice, we compared the relative intensity of a pristine Mn_{II} and satellite Mn_{IInew} lines with the calculated probability of having

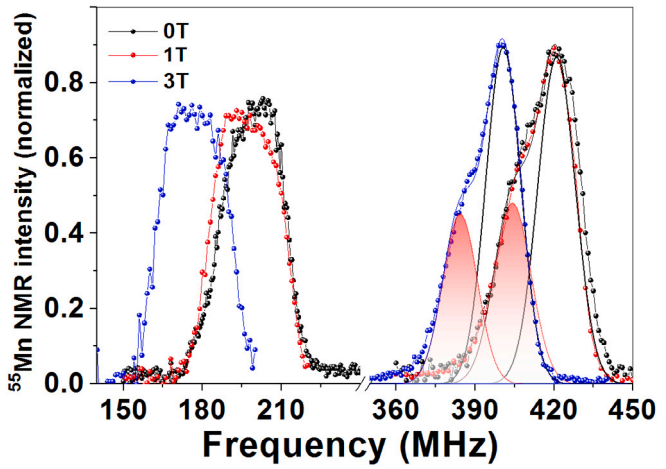

Fig. 9. ^{55}Mn NMR spectra recorded from the $Mn_5(Ge_{0.6}Si_{0.4})_3$ film in the external out-of-plane fields of 0, 1 and 3 T. Red shaded areas indicate the Mn_{IInew} satellite line.

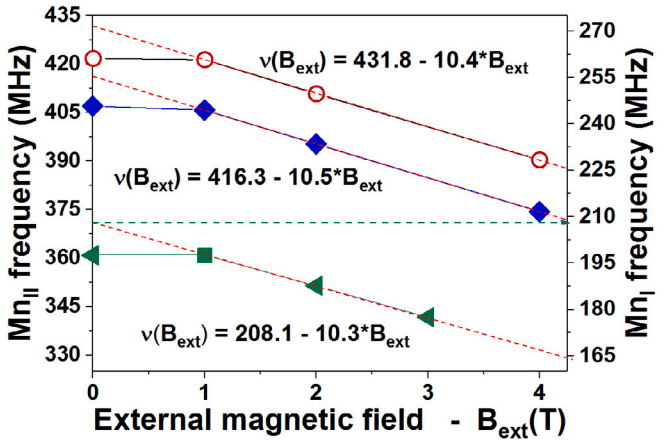

Fig. 10. Frequency of the central NMR lines from: Mn_I (green triangles), Mn_{II} (open red circles) and Mn_{IInew} (blue squares) manganese sites as a function of the external out-of-plane field.

a given number of Si neighbors in those environments at different Si concentrations. As shown in the Fig. 11 the relative contribution of the Mn_{IInew} satellite to the total spectrum intensity coincides with a probability of finding 2 Si neighbors around the Mn_{II} site, showing that the reduced magnetic moment is observed for those Mn_{II} atoms that have at least two Si neighbors instead of Ge.

With increasing Si concentration, the population of pristine Mn_{II} environments drops down and consequently the average magnetic moment decreases – this "background" effect accounts for a progressive downshift of the original NMR lines, in both manganese lattices.

Our previous NMR investigations of a pristine Mn_5Ge_3 film have shown that manganese in the 6(g) site reveals a considerable anisotropy of hyperfine fields not only between the *c*-axis and c-plane, but also within the hexagonal c-plane. Due to the in-plane anisotropy, a hyperfine field at each of the hexagonally arranged Mn_{II} sites has an ellipsoidal, rather than spherical symmetry. Therefore each of the three Mn_{II} atoms that are located at the same plane in a unit cell, contributes a different, angle-dependent component to a cumulative NMR spectrum. As a result, the shape of the NMR spectra recorded in presence of an in-plane magnetic field varies as a function of the φ angle within the c-plane. In particular, for specific in-plane directions the NMR spectra displayed a well resolved doublet structure [12,14]. To find out whether the Si/Ge substitution affects the in-plane anisotropy of the

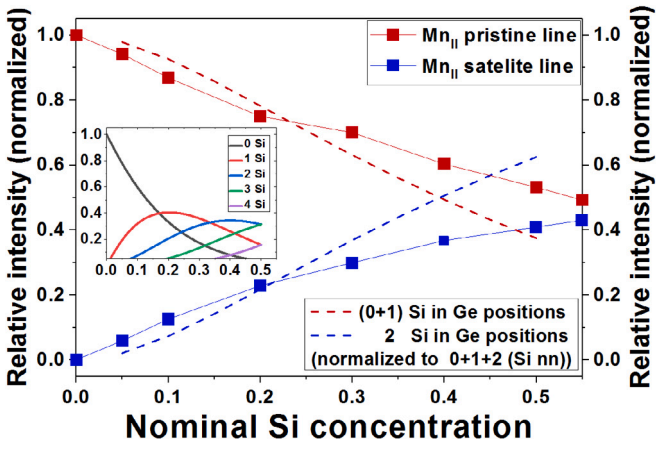

Fig. 11. Relative intensity of a pristine Mn_{II} and satellite Mn_{IInew} NMR line as a function of Si concentration. Inset: the calculated probability of Mn_{II} atom having 0, 1, 2, 3 or 4 Si neighbors.

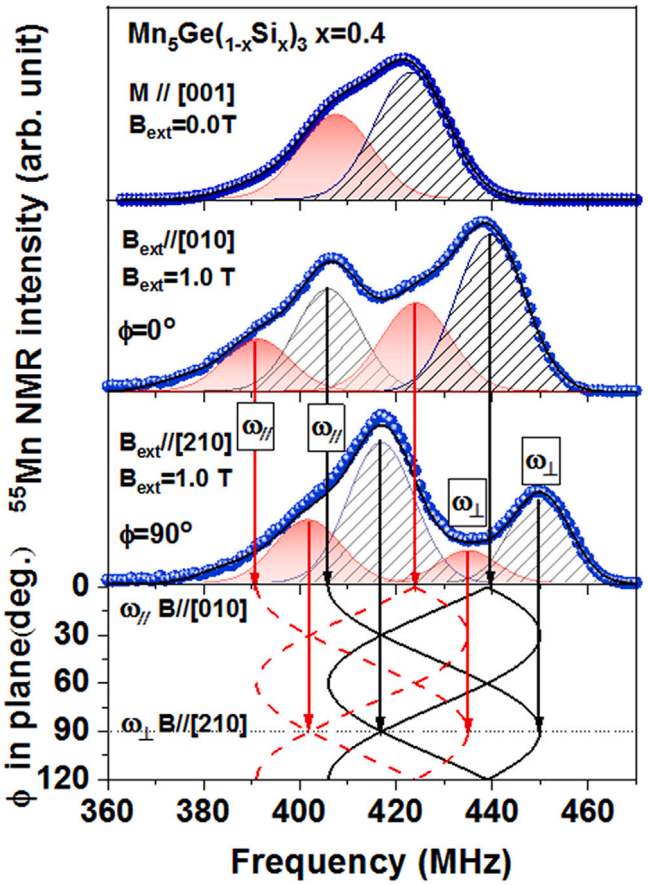

Fig. 12. ^{55}Mn NMR spectra from the Mn_{II} site recorded at 4.2 K: a) at zero field, i.e. along [001] axis; (b) external magnetic field along [010]; (c) external magnetic field along [210]. Hatched areas denote the signals from pristine Mn_{II} environments, and red shaded areas are from the Mn_{IInew} environments. Bottom panel: NMR frequency as a function of orientation of the in-plane field, computed for three nonequivalent Mn_{II} positions (n = 1, 2, 3) located on the same atomic plane (z = 1/4): $\nu_n(\varphi) = \nu_0 + \Delta\nu sin^2(\varphi + (n-1)60)$.

Mn_{II} hyperfine field, we performed a similar experiment on a film with $x = 0.4$. Fig. 12 shows the NMR spectra from the Mn_{II} site recorded from the $Mn_5(Ge_{0.6}Si_{0.4})_3$ film along the [001] direction (hexagonal c-axis), i.e. the zero-field spectrum, as well as for the two respective in-plane directions: [010] and [210]. The spectra have been decomposed

using the Gaussian line shapes. The decomposition shows that the two main components of the NMR spectrum: a pristine Mn_{II} line (hatched areas) and the Mn_{IInew} satellite (red shaded areas), each become split into a doublet for the in-plane [010] direction ($\varphi = 0°$) as well as for the [210] ($\varphi = 90°$). A frequency position of the respective doublet components makes it possible to calculate the in-plane anisotropy. Denoting the frequency at $\varphi = 0°$ as ν_0 and a difference between ν_0 and a frequency corresponding to $\varphi = 90°$ as $\Delta\nu$, it can be shown that the angular dependence of NMR frequency $\nu_n(\varphi)$ for each of the three Mn_{II} atoms located on the same plane (n = 1, 2, 3) is described by the following formula [12].

$$\nu_n(\varphi) = \nu_0 + \Delta\nu sin^2(\varphi + (n-1)60) \quad (4)$$

Entering the experimental values of ν_0 and $\Delta\nu$ into the formula (2), the respective plots of the NMR frequency versus the in-plane field orientation have been computed for each of the nonequivalent Mn_{II} atoms (n = 1, 2, 3) in Mn_5Ge_3 and $Mn_5(Ge_{0.6}Si_{0.4})_3$ films and all are presented the bottom panel in Fig. 12. The amplitude of each sinusoidal function is a measure of the in-plane anisotropy of hyperfine fields in a given Mn_{II} site. Obviously, due to the in-plane variation of hyperfine field value the anisotropy measured between the c-plane and c-axis depends on the in-plane direction. As shown in Fig. 12 the amplitude is the same for both, the Mn_{II} environments in a pristine Mn_5Ge_3 and in the $Mn_5(Ge_{0.6}Si_{0.4})_3$ film (Mn_{II} as well as Mn_{IInew} sites) and amounts to around 4 T. This analysis shows that the Mn_{II} atoms having Si in the nearest environment retain almost unchanged anisotropy of the orbital moment, in spite of a sharply decreased value of the magnetic moment. The uniform shift between the respective sinusoids gives an additional evidence that the Mn_{II} and Mn_{IInew} environments are ferromagnetically coupled.

4. Conclusions

In conclusion, using the frequency of ^{55}Mn NMR lines as fingerprints of specific magnetic environments we have identified a new population of the 6(g) manganese sites (denoted as Mn_{IInew}), distinguished by a lower magnetic moment, that coexist with the unaltered Mn_{II} environments (having the same properties as those observed in the pristine Mn_5Ge_3 film). A similar new NMR signal at a frequency just below the Mn_{II} peak (denoted as LH signal) has been also observed in polycrystalline alloys of $Mn_5(GeSi)_3$ [10]. Based on the comparison of signal intensities the authors of Ref. [10] assigned this new LH signal to the modified Mn_I environments. However, this assignment is not tenable in view of the new information brought by the experiments on epitaxial films reported in the presented paper. The increasingly asymmetric shape of the Mn_{II} spectra as a function of Si concentration (cf. Fig. 7) intuitively suggests to consider the new structure as a satellite of the Mn_{II} signal. This attribution is fully confirmed by the anisotropy of hyperfine fields evidenced by the experiments in presence of the external magnetic field. In the Mn_{IInew} environments hyperfine fields display characteristics identical to those in the pristine Mn_{II} (cf. Fig. 9 and Fig. 12), and distinctly different from the behavior of the Mn_I line, which is dominated by the quadrupolar effects (cf. Fig. 5). In other words, a thorough analysis of the NMR experiments performed at 4.2 K on a series of mixed $Mn_5(Ge_{1-x}Si_x)_3$ ($0 \leqslant x \leqslant 0.55$) films shows that a substitution of Ge with Si affects primarily the magnetic properties of manganese in the 6(g) lattice sites, which are located in the same plane as Ge/Si.

The onset of the low-moment Mn_{IInew} environments at the expense of pristine Mn_{II} is reflected in a progressive drop of the average saturation magnetic moment with increasing Si concentration. This was observed in the polycrystalline $Mn_5(GeSi)_3$ alloys [18] and recently in the epitaxial films, where this effect is even strongly enhanced with respect to the bulk specimens [9]. The interpretation given in Ref. [18], attributes this effect to a mixing of the 3d electron states of Mn with the 3p electron states of Si atoms. This additionally supports the attribution of the low-moment states to the 6(g) sublattice, where the interatomic distances between the Mn atoms and Ge/Si sites are shorter than in the 4(d) sublattice and thus more prone to experience the effect of the orbital overlay. Furthermore we show that the number of the Mn_{IInew} environments coincides with a probability of finding two Si atoms instead of Ge in the nearest neighborhood of a 6(g) site. The 4(d) environments are not significantly altered by Si substitution in the studied concentration range. The effect of Si on the Mn_I atoms is secondary and consists in a smaller contribution of the transferred hyperfine field due to the reduced magnetic moment of the Mn_{IInew} neighbors and a certain EFG inhomogeneity brought about by a local lattice distortion due to Ge/Si replacement. Interestingly, a significant anisotropy of the orbital moment is preserved in all manganese sites for all studied concentrations.

The effects of Ge replacement with Si in the $Mn_5(GeSi)_3$ epitaxial alloys can be regarded as a first step towards creating a low-temperature AF1 structure reported in Mn_5Si_3 films (i.e. $x = 1$). Coexistence of Mn_{II} and Mn_{IInew} environments in the mixed concentration region, indicates that a transition from the FM order for $x = 0$ to AF1 structure for $x = 1$ represents a first order phase transition.

CRediT authorship contribution statement

R. Kalvig: Investigation, Validation, Formal analysis, Visualization. **E. Jędryka:** Conceptualization, Methodology, Writing – original draft, Writing – review & editing. **S. Kang:** Investigation, Resources. **M. Petit:** Resources. **L. Michez:** Resources. **M. Wójcik:** Methodology, Formal analysis, Visualization, Supervision.

Declaration of competing interest

The authors declare that they have no known competing financial interests or personal relationships that could have appeared to influence the work reported in this paper.

Data availability

Data will be made available on request.

Acknowledgments

This article is based upon work from COST-OPERA Action CA20116, supported by COST (European Cooperation in Science and Technology). The materials growth was supported by the French national research agency (ANR) and the Deutsche Forschungsgemeinschaft (DFG), Germany (Project MATHEEIAS - Grant No. ANR-20-CE92-0049-01 / DFG-445976410) and by a French government grant managed by the Agence Nationale de la Recherche, France under the France 2030 program (ANR-22-EXSP-0007).

References

[1] C. Surgers, G. Fischer, P. Winkel, H.v. Löhneysen, Nature Commun. 5 (2014) 3400.
[2] N. Biniskos, K. Schmalzl, S. Raymond, S. Petit, P. Steffens, J. Persson, T. Brückel, Phys. Rev. Lett. 120 (2018) 257205.
[3] M. Leiviskä, J. Rial, A. Badura, R.L. Seeger, I. Kounta, S. Beckert, D. Kriegner, I. Joumard, E. Schmoranzerová, J. Sinova, O. Gomonay, A. Thomas, S.T.B. Goennenwein, H. Reichlová, L. Šmejkal, L. Michez, T. Jungwirth, V. Baltz, arXiv:2401.02275.
[4] L. Šmejkal, J. Sinova, T. Jungwirth, Phys. Rev. X 12 (2022) 040501.
[5] I. Kounta, H. Reichlová, D. Kriegner, R.L. Seeger, A. Badura, M. Leiviskä, A. Boussadi, V. Heresanu, S. Bertaina, M. Petit, E. Schmoranzerová, L. Šmejkal, J. Sinova, T. Jungwirth, V. Baltz, S.T.B. Goennenwein, L. Michez, Phys. Rev. Math. 7 (2023) 024416.
[6] N. Biniskos, F.J. dos Santos, K. Schmalzl, S. Raymond, M. dos Santos Dias, J. Persson, N. Marzari, S. Blügel, S. Lounis, T. Brückel, Phys. Rev. B 125 (2022) 104404.
[7] G. Kappel, G. Fischer, A. Jaéglé, Phys. Status Solidi. 34 (1976) 691.

[8] Ch. Zeng, S.C. Erwin, L.C. Feldman, A.P. Li, R. Jin, Y. Song, J.R. Thompson, H.H. Weitering, Appl. Phys. Lett. 83 (2003) 5002.
[9] S. Kang, M. Petit, V. Heresanu, A. Altié, T. Beaujard, G. Bon, O. Cespedes, B. Hickey, L. Michez, Thin Solid Films 797 (2024) 140338.
[10] P. Panissod, A. Qachaou, G. Kappel, J. Phys. C: Solid State Phys. 17 (1984) 5799.
[11] P. Panissod, M. Malinowska, E. Jedryka, M. Wojcik, S. Nadolski, M. Knobel, J.E. Schmidt, Phys. Rev. B 63 (2001) 014408.
[12] R. Kalvig, E. Jedryka, M. Wojcik, M. Petit, L. Michez, Phys. Rev. B 101 (2020) 094401.
[13] K. Momma, F. Izumi, J. Appl. Crystallogr. 44 (2011) 1272.
[14] R. Kalvig, E. Jedryka, M. Wojcik, G. Allodi, R. De Renzi, M. Petit, L. Michez, Phys. Rev. B 97 (2018) 174428.
[15] R.E. Watson, A.J. Freeman, Phys. Rev. 123 (1961) 2027.
[16] J.B. Forsyth, P.J. Brown, J. Phys.: Condens. Matter. 2 (1990) 2713.
[17] M.H. Cohen, F. Reiff, Nuclear quadrupole effects in solids, in: Solid State Physics, vol. 5, Academic, New York, 1957, p. 321.
[18] F.Q. Zhao, W. Dagula, O. Tegus, K.H.J. Buschow, J. Alloy. Compd. 416 (2006) 43.